River Flow 2010 - Dittrich, Koll, Aberle & Geisenhainer (eds) - © 2010 Bundesanstalt für Wasserbau ISBN 978-3-939230-00-7

Simultaneous Measurements of Concentration and Velocity with Combined PIV and planar LIF in Vegetated Open-Channel Flows

Taka-aki Okamoto, Iehisa Nezu & Aki Katayama
Department of Civil Engineering, Kyoto University, Kyoto 615-8540, Japan

ABSTRACT: Aquatic plants reduce suspended sediment transport because of the local reduction in bed shear stress. Therefore, it is very important for river environment to reveal the mass and momentum exchanges near the vegetation zone. Turbulent diffusion mechanisms in emergent vegetated flows have recently been investigated by many researchers. However, the effect of the submerged vegetation on the scalar flux has not been fully investigated. So, continuous dye injection experiments were conducted to evaluate the vertical mass transport in open-channel flow with rigid vegetation models by changing the vegetation density. In the present study, a combination technique between PIV and planar laser-induced fluorescence (LIF) was developed by using two sets of CMOS cameras, to measure the instantaneous velocity and the instantaneous concentration field simultaneously.

Keywords: LIF, PIV, Simultaneous measurements, Submerged vegetation, Vertical scalar flux

1 INTRODUCTION

Aquatic plants are fundamental components of a natural water environment in rivers and wetlands. Submerged vegetation generates coherent turbulent motions near the vegetation edge and reduces suspended sediment transport because of the local reduction in bed shear stress. It is therefore important for river management to investigate hydrodynamic characteristics and coherent eddies in open-channel flows with vegetation canopies. In recent years, the measuring techniques of PIV and planar laser induced fluorescence (LIF) are extensively used to investigate the mixing processes.

For example, Chen & Jirka (1999) have measured the instantaneous concentration field in shallow jet flows by LIF. They revealed the overall meandering of the plane jet and the role of large-scale turbulence structure in the mixing processes.

Crimaldi & Koseff (2001) measured the spatial and temporal structure of an odor plume in turbulent flows by two kinds of LIF techniques, i.e., full-field planar LIF and single-point LIF probe. The results showed a wide range of turbulent structures in detail; the nature of the structure varied significantly in the different regions of plume.

Rahman & Webster (2005) conducted planar LIF measurements in turbulent open-channel flow and examined the effect of bed roughness on a chemical plume. They revealed that the concentration fluctuation intensity is smaller and decreases faster as the bed roughness increases.

On the other hand, turbulence structure and transport mechanism of momentum and mass in the vegetated flows have been investigated in the past decades. Gao et al. (1988) have proposed a ramp-jump structure and humidity within and above a terrestrial canopy by using triaxial sonic anemometers and thermometer. They revealed that coherent structures consisted of a weak ejection from the canopy top followed by a strong sweep into the canopy.

Ghisalberti & Nepf (2005) conducted continuous dye injection experiments to characterize vertical mass transport in submerged vegetation flow. Through the absorbance-concentration relationship of the Beer Lambert law, a digital imaging was used to provide high-resolution concentration profiles of the dye plumes. They suggested that vertical mass transport has the strong periodicity and coherent vortices of the shear layer dominate the turbulent diffusion.

Reidenbach et al. (2007) have measured fine-scale mixing and mass transport within a coral canopy by using planar LIF. They showed that the action of surface waves, interacting with the struc-

Table1 Hydraulic condition

Case	Φ	H(cm)	h (cm)	H/h	U_m(cm/s)	Re	Fr
R1	0.0	15.0	-	-	12.0	30000	0.17
R2	0.015		5.0	1.0			
R3	0.061						

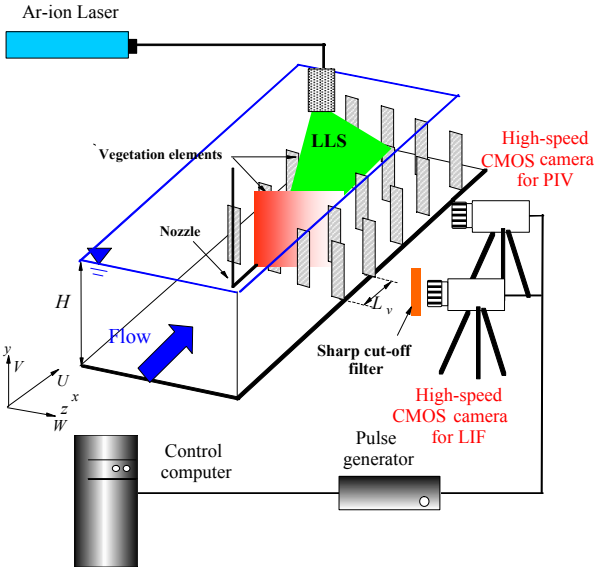

Figure 1 Experimental set-up

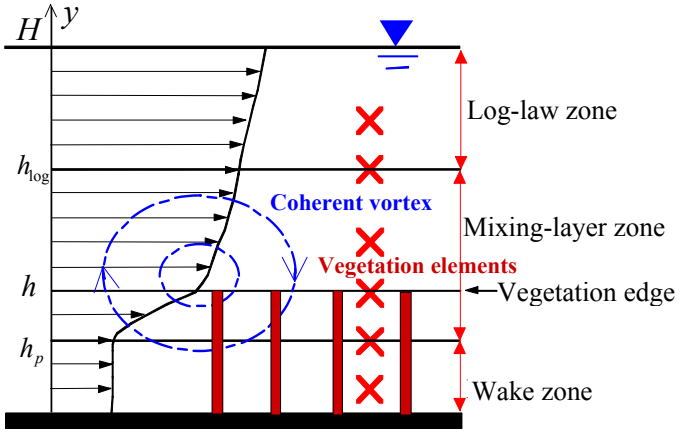

Figure 2 Flow zone model in vegetated open-channel flow

ture of the reef, could increase instantaneous shear and mixing up to six times compared to that of non-conditional flow.

Jamali et al. (2008) conducted LIF measurements to investigate the exchange flow due to the temperature differences between the vegetation and non-vegetation zones. They suggested that the magnitude of the exchange rate decreases as the canopy drag increases.

However, these above-mentioned previous studies do not offer the detailed information of turbulent diffusion mechanism, because it has been difficult to measure the velocity and concentration fluctuations simultaneously. In the present study, a combination technique between PIV and LIF was developed by using two sets of high-speed cameras to measure the instantaneous velocity and instantaneous concentration field simultaneously. Of particular significance is that that the synchronicity allows the direct computation of scalar flux and velocity. Consequently, effects of coherent vortices on scalar flux were examined in detail.

2 EXPERIMENTAL METHOD

2.1 *Experimental setup and vegetation model*

The experimental setup and the coordinate system are indicated in Figure 1. The present experiments were conducted in a 10m long and 40cm wide tilting flume. x, y and z are the streamwise, vertical and spanwise coordinates, respectively. H is the water depth and h is the vegetation height. B_v and L_v are the neighboring vegetation spacings in the spanwise and streamwise directions, respectively. The elements of vegetation model were made of rigid-strip plates (h=50mm height, b=8mm width and t=1mm thickness) in the same manner as conducted in laboratory experiments by Nezu & Sanjou (2008). The time-averaged velocity components in each direction are defined as U, V and W, and the corresponding turbulent fluctuations are u, v and w, respectively. $\tilde{c}(t) \equiv C + c(t)$ is the instantaneous dye concentration, which is defined in the same manner as velocity components.

In the present study, a combination technique between PIV and laser-induced fluorescence (LIF) was developed by using two sets of CMOS cameras (1024×1024 pixels), to measure the instantaneous velocity components $(\tilde{u}, \tilde{v})$ and the instantaneous concentration $\tilde{c}$ simultaneously. The 2mm thickness laser-light sheet (LLS) was generated by 3W Argon-ion laser. The illuminated flow pictures were taken by two sets of high-speed cameras with 500Hz frame-rate and 60s sampling time. The instantaneous velocity components $(\tilde{u}, \tilde{v})$ on the x-y plane were analyzed by the PIV algorithm for the whole flow depth region. These PIV methods are the same as used previously by Nezu & Sanjou (2008).

The instantaneous concentration field $\tilde{c}(x, y)$ was quantified by using the planar LIF technique. Dye (Rhodamine B) was injected through a 3mm diameter stainless nozzle. The

dye-injection velocity was adjusted to match the local flow velocity U. The dye absorbed the green laser light and reemitted light with the different longer wavelengths. Under appropriate conditions, the light intensity emitted by the dye is directly proportional to the dye concentration and laser light intensity. Consequently, the planar concentration field $\tilde{c}(x,y,t)$ is calculated from the captured images by one CMOS camera (for LIF), using a relevant calibration function.

2.2 *Hydraulic condition*

Table 1 shows the hydraulic condition. The bulk mean velocity U_m and the submergence depth H/h were kept constant for all cases, i.e., $U_m = 12$ cm/s and H/h=3.0. Two kinds of experiments were conducted by changing the vegetation density Φ and the vertical position of the nozzle tip y_0. In this study, the vegetation density Φ is defined as follows:

$$\Phi = \frac{\sum_i A_i b_i}{S \cdot h} = ab \qquad (1)$$

in which, A_i is the frontal area of the vegetation element, b_i is the vegetation-element width and S is the referred bed area.

In the present study, the nozzle tip position was changed to examine the turbulent diffusion properties in all three sub-zones of the vegetated open-channel flow, as shown in Figure 2

Nepf & Vivoni (2000) and Poggi et al.(2004) have pointed out that the whole depth region in submerged vegetation flow could be classified into several layers on the basis of the vertical profiles of mean streamwise velocity and Reynolds stress. Nezu & Sanjou (2008) found that the submerged rigid canopy flow can be divided into the following three sub-zones on the basis of previous experimental results.

$$\left.\begin{array}{l} \textit{Wake zone}\ \left(0 \le y \le h_p\right) \\ \textit{Mixing-layer zone}\ \left(h_p \le y \le h_{\log}\right) \\ \textit{Log-law zone}\ \left(h_{\log} \le y \le H\right) \end{array}\right\} \qquad (2)$$

h_p is the penetration depth defined by Nepf & Vivoni (2000) and $h_{\log}$ is the lower limit of the log-law zone defined by Nezu & Sanjou (2008). In the Wake zone ($0 \le y \le h_p$), the vertical turbulent momentum transport is negligibly small due to the strong wake effects behind vegetation stems, i.e. the Karman vortex appears predominately. In the Mixing-layer zone ($h_p \le y \le h_{log}$), a large-scale coherent vortex is generated near the vegetation edge due to the inflection-point instability and consequently, the vertical turbulent exchange contributes largely to the momentum transfer between over- and the within-canopies, as discussed by Raupach et al. (1996) for terrestrial canopy, and by Nezu & Sanjou (2008) for aquatic canopy. h_{log} is the lower limit position of the Log-law zone, in which turbulence characteristics are analogous to those of boundary layers.

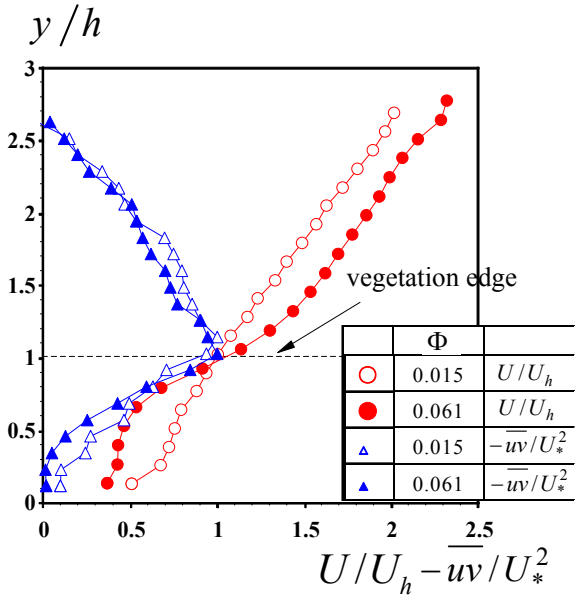

Figure 3 Mean velocity and Reynolds stress

3 RESULTS

3.1 *Mean flow*

Before examinations of the concentration field, it is very important to examine the mean-flow and turbulence characteristics in vegetated open-channel flows. Figure 3 shows the vertical distributions of the time-averaged and space- (horizontal) averaged (i.e. double-averaged) streamwise velocity U and Reynolds stress $-uv$ for submerged vegetation density (Φ =0.015, 0.061). These values are normalized by the mean velocity at the vegetation-edge U_h and the friction velocity U_*, respectively. The value of U_* was evaluated as the peak of $-uv$ in the same way as conducted by Nezu & Sanjou (2008). Near the top of the vegetation (y/h=1.0), both the local velocity $U(y)$ and its gradient $\partial U/\partial y$ increase rapidly, which induces a strong shear layer and a significant inflection-point instability, as pointed by many researchers.

It should be noticed that the value of $-\overline{uv}$ attains maximum near the vegetation edge, i.e., y/h=1.0. The Reynolds stress decays rapidly in the canopy layer (y/h<1) and becomes negligibly small near the channel bed. Figure 3 also shows that the values of Reynolds stress decrease with an increase of the vegetation density Φ.

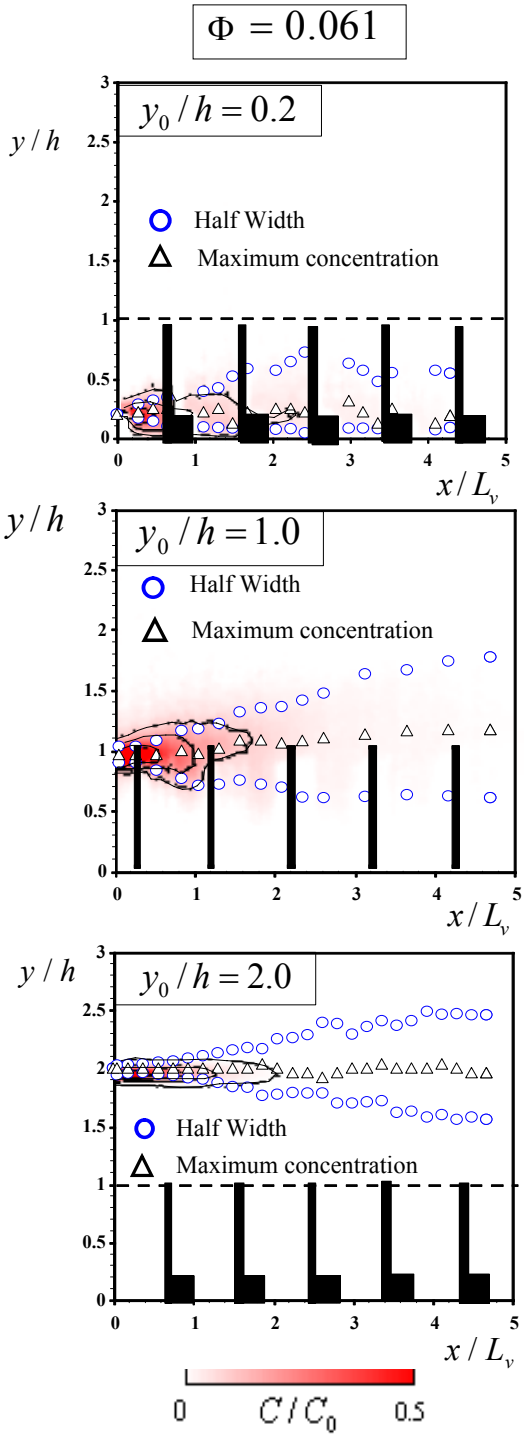

Figure 4 Contours of time-averaged concentration

3.2 *Time-averaged concentration*

Figure 4 shows the contour lines of the time-averaged dye concentration $C(x, y)$ for Φ=0.061 (dense canopy). The nozzle tip positions are y_0/h = 0.2 (Wake zone), 1.0 (Mixing-layer zone) and 2.0 (Log-law zone). The contour values are normalized by the mean concentration at the nozzle tip C_0. To evaluate the vertical turbulent diffusion quantitatively, the streamwise variations of the half-value-width $b_{1/2+}$ (upper layer) and $b_{1/2-}$ (lower one) as well as the trajectory of the maximum concentration $C_{\max}$ are also included in Figure 4. It is found clearly that the plume evolves downstream and the half-value-widths $b_{1/2+}$ and $b_{1/2-}$ increase linearly along the x-axis, which is consistent with the experiments of Webster et al. (2003).

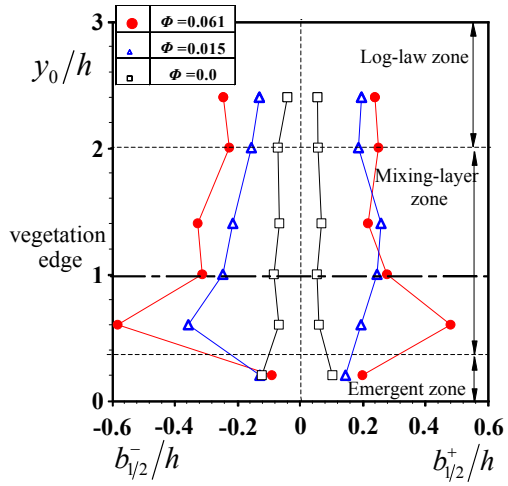

Figure 5 Distribution of half-value-width (x/L_v = 2.0)

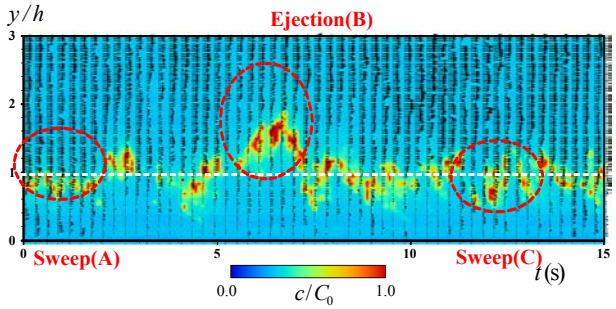

Figure 6 Time series of instantaneous velocity vectors and concentration field

Figure 5 compares the half-value-width $b_{1/2+}$ and $b_{1/2-}$ at x/L_v=2.0 for Φ=0.0, 0.015 and 0.061. Both of $b_{1/2+}$ and $b_{1/2-}$ become larger at y_0/h=0.6 and 1.0, i.e., in the Mixing-layer zone, for Φ=0.015 and 0.061. The vertical turbulent diffusion is smaller at y_0/h=0.2, i.e., in the Wake zone and y_0/h=2.4, i.e., in the Log-law zone. In contrast, for the Smooth flat bed (no vegetation, Φ=0.0), the values of $b_{1/2+}$ and $b_{1/2-}$ are negligibly small, irrespective of the nozzle tip position of y_0/h. This implies that in submerged vegetation flows, a large-scale coherent vortex is generated near the vegetation edge due to the inflection-point instability (Figure 3) and the vertical turbulent exchange contributes largely to the scalar transport in the Mixing-layer zone. These results are in good agreement with Nepf & Vivoni (2000) and Nezu & Sanjou (2008).

It is also observed that $b_{1/2+}$ and $b_{1/2-}$ for Φ=0.061 (dense canopy) are greater than those for Φ =0.015 (sparse canopy) and Φ =0.0 (smooth bed). Nezu & Sanjou (2008) pointed out that the strong shear layer appears near the vegetation edge for dense canopies. Ghisalberti & Nepf (2005) also demonstrated that the dense canopies would generate vortices with a greater rotational speed and that the higher rates of rotation would result in a more rapid flushing in the canopy layer. Therefore, it is recognized that the large distributions of the dye concentration are mixed rapidly due to the strong shear layer for Φ=0.061.

3.3 *Instantaneous velocity and concentration field*

Figure 6 shows the time-series of instantaneous velocity vectors $(\tilde{u},\tilde{v})$ by PIV and the corresponding instantaneous concentration field $\tilde{c}(x,y,t)$ by LIF. At t = 0.0s, a sweep motion is observed below the canopy top. The dye concentration is transported into the canopy layer. At t = 6.0-7.0s, an ejection motion appears and the high value of concentration is observed above the vegetation edge. At t = 12.0-13.0s, the sweep motion appears again near the vegetation top.

Figure 7 shows some examples of the instantaneous velocity vectors $(\tilde{u},\tilde{v})$, which were ob-

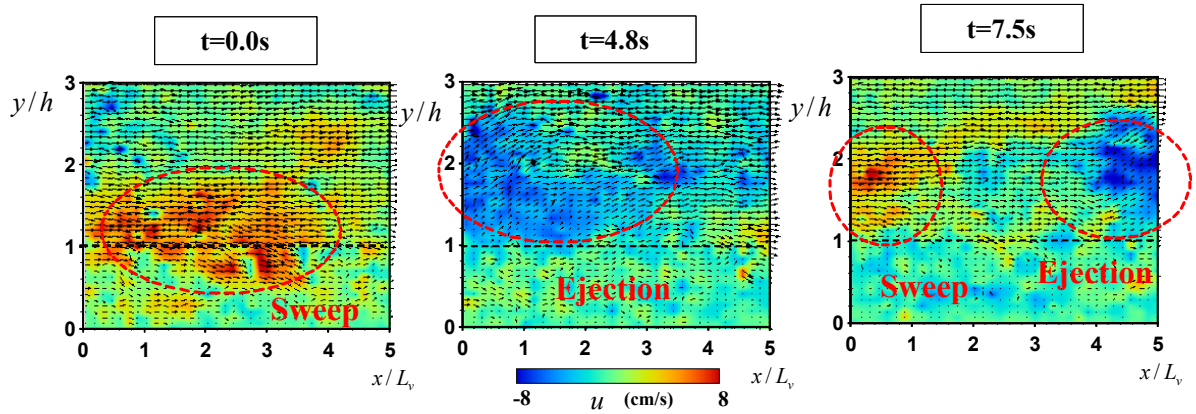

Figure 7 Instantaneous velocity vectors

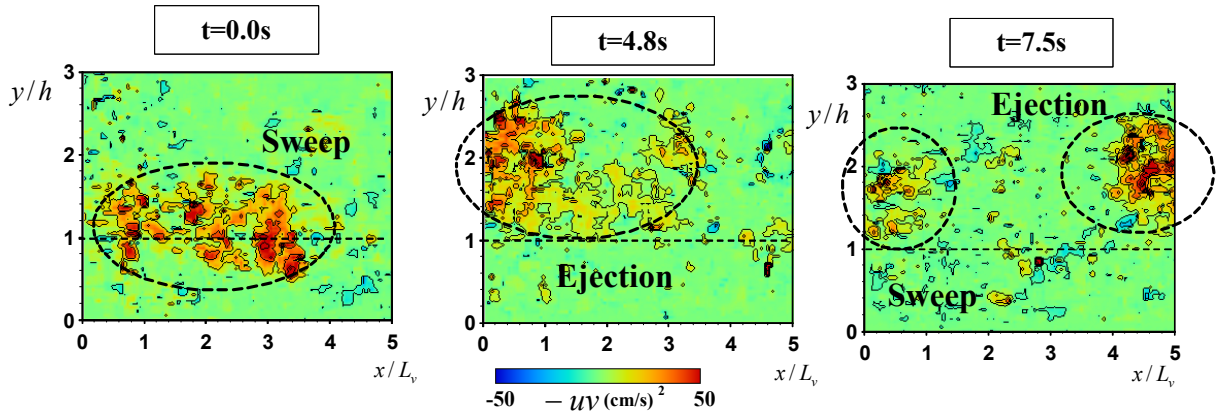

Figure 8 Instantaneous Reynolds stress

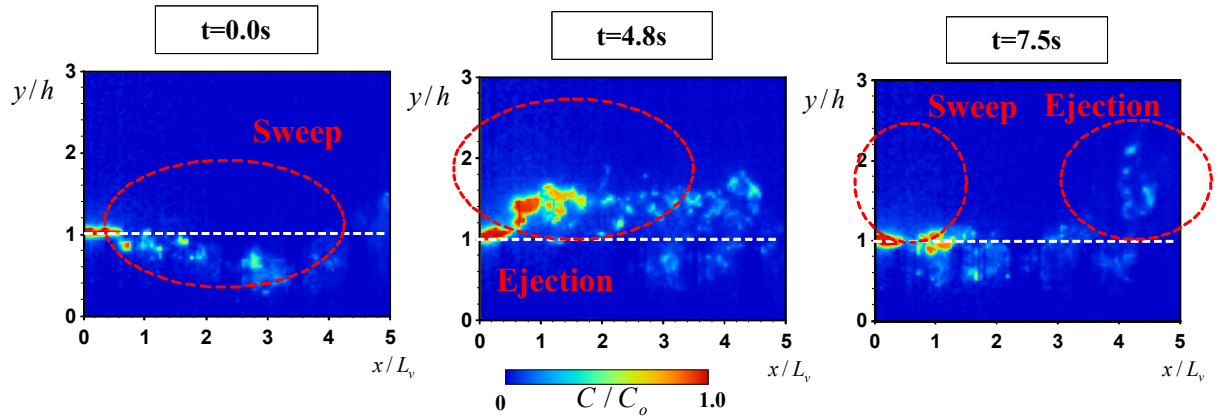

Figure 9 Corresponding instantaneous concentration field

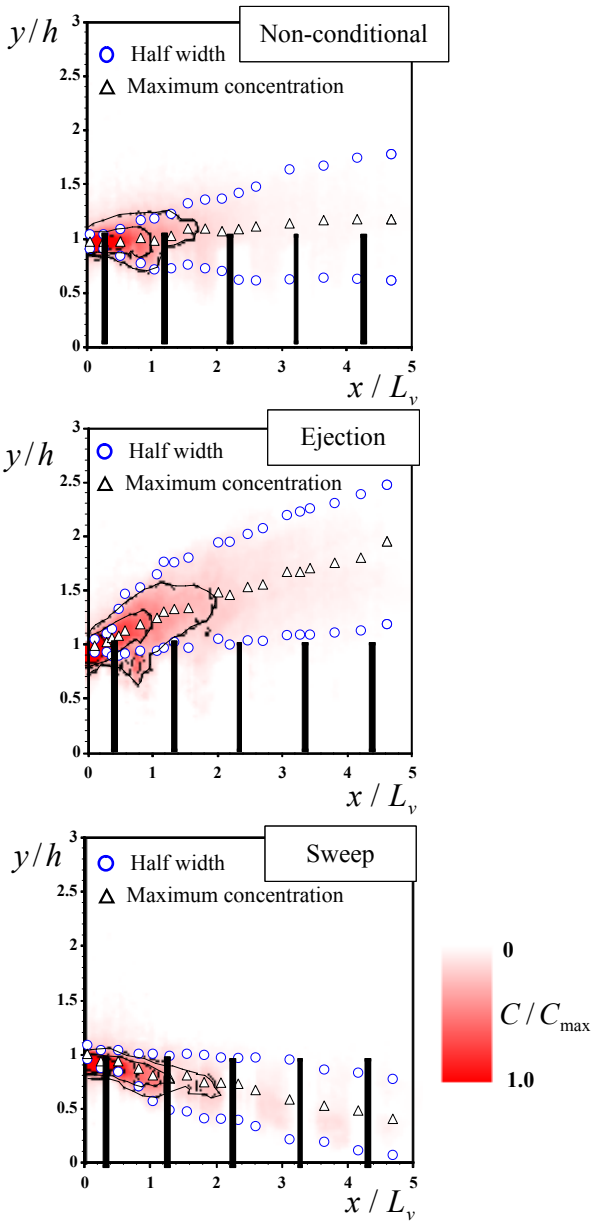

Figure 10 Contour of conditional sampling concentration

tained by PIV. The contours indicate the magnitude of turbulent fluctuations u (x,y,t) for the streamwise velocity component. Figure 8 shows the contours of the instantaneous Reynolds stress $-u(t)v(t)$ at the same time. It is recognized that large values of the instantaneous Reynolds stress are located near the vegetation edge and these locally-high distributions of Reynolds stress correspond well to ejection and sweep motions of Figure 7. These results imply that the coherent motions govern the momentum transfer near the canopies significantly. These noticeable features for submerged canopies are in good agreement with Nezu & Sanjou (2008).

Figure 9 shows the corresponding simultaneous concentration field $c(x,y,t)$ measured by LIF. Figure 9 reveals the high spatial variability of the instantaneous concentration field. At t=0.0(s), a sweep motion, i.e., the downward vectors, appears near the vegetation edge. It is observed that the large distribution of the instantaneous concentration is transported downward $(v<0)$ by the sweep motion. At t=4.8(s), an ejection motion is observed and causes the local increase of the concentration above the canopy. At t=7.5(s), the ejection motion is transported downstream and the other sweep motion appears at the upstream side. The individual filaments of the dye concentration are observed clearly and the highly intermittent nature of the plume is exhibited, which is consistent with Rahman & Webster (2005). These images also show that the locally-high distributions of dye concentration correspond well to these coherent structure zones.

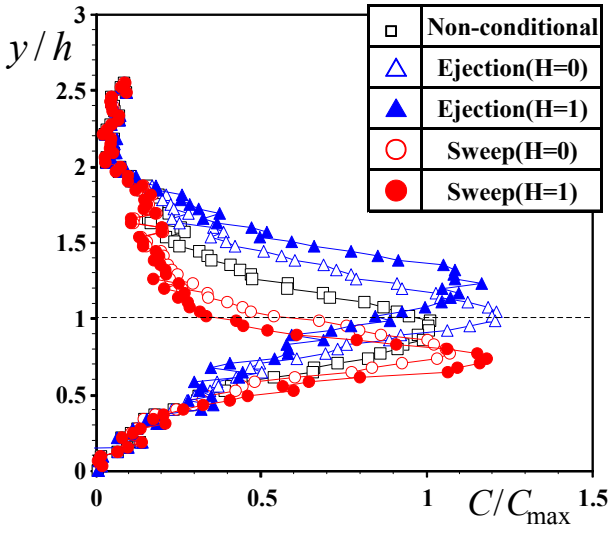

Figure 11 Distribution of conditional sampling concentration

These results provide more evidence that the large-scale coherent motions dominate the vertical mass and momentum transport in vegetated flows.

3.4 *Conditional analysis*

To examine the effects of the coherent motions on the vertical turbulent diffusion quantitatively, quadrant analyses were performed. Figure 10 (b) and (c) show the contours of the concentration C_E and C_S at y_0/h=1.0 for ϕ=0.061 (dense canopy) by using conditional sampling of the Ejection motion (u<0, v>0) and the Sweep motion (u>0, v<0), respectively. The contour of the time-averaged concentration (non-conditional) C is also included for comparison in Figure 10(a). It is evident from Figure 10 (b) that C_E has the peak value above the vegetation edge and the values of C_E are larger than C (non-conditional) over the canopy. This implies that the high-value of the dye concentration is transported to the above-canopy layer by the Ejection motion, which is consistent with Figs.4 and 5. Whereas, C_S becomes larger than C below the vegetation edge and the Sweep motion transports the dye concentration into the within-canopy layer.

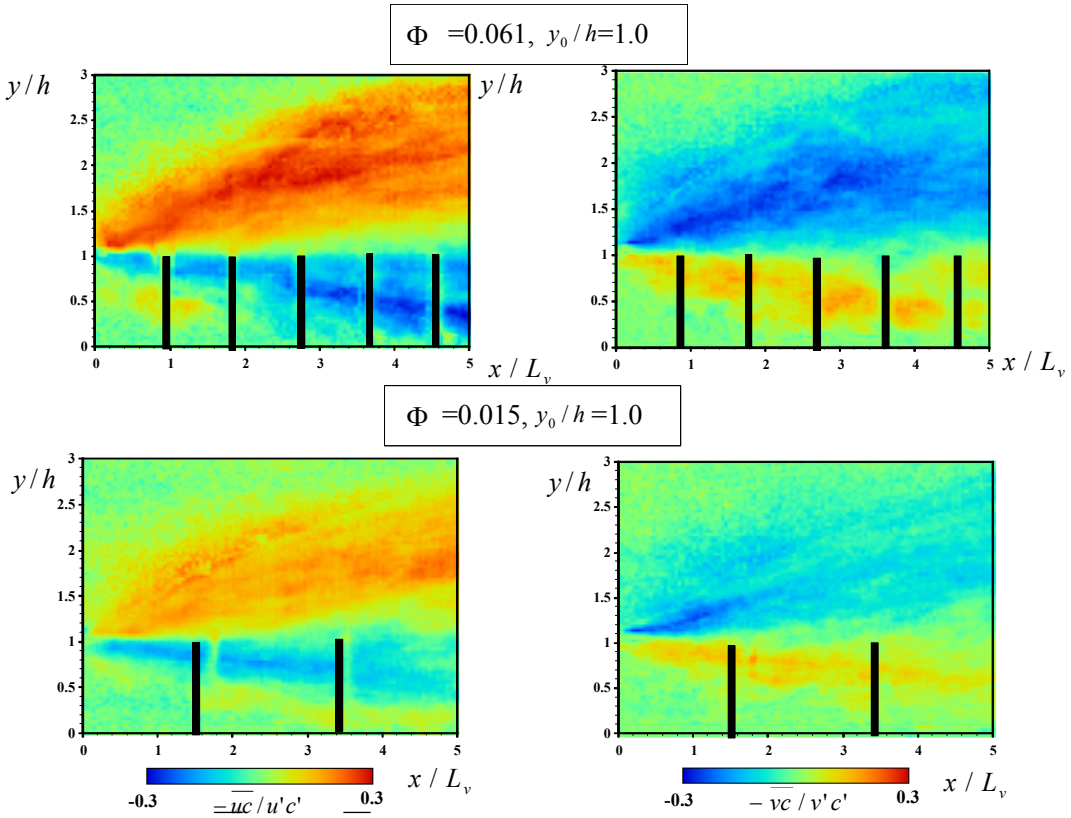

Figure 12 Turbulent scalar flux $-uc$ and $-vc$ (y_0/h=1.0)

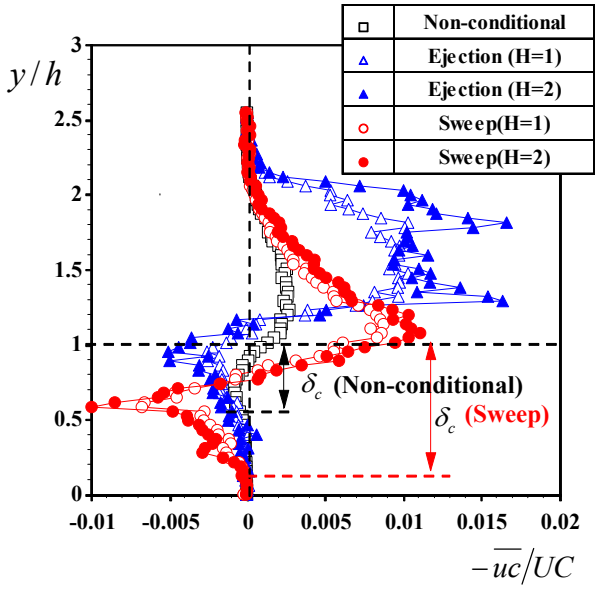

Figure 13 Vertical distribution of conditional sampling turbulent scalar flux (ϕ=0.061)

Figure 11 shows the vertical distributions of the concentration C_E and C_S at y_0/h=1.0 for Φ=0.061 by using conditional sampling of the Ejections and Sweeps. To exclude the less-organized motion, a threshold level H, so-called the 'hole-value' is used. The values of the concentration $C_E(H=1)$ and $C_S(H=1)$ are greater than those of $C_E(H=0)$ and $C_S(H=0)$. This indicates that much organized Sweep and Ejection motions would transport larger-values of the dye concentration.

It is also observed that the value of C_S decreases more rapidly than that of C_E, which is consistent with Figure 10. These results reveal that the large distributions of the dye concentration are mixed more rapidly within the canopy due to the stronger wake effects behind vegetation stems, and consequently, the peak value of C_S decreases more significantly in the within-canopy layers.

3.5 Turbulent *scalar* flux

Of particular significance in this study is the turbulent scalar flux of a passive tracer. The PIV-LIF measurements afford us to calculate the local covariance between the concentration and velocity fluctuations, $-uc$ and $-vc$. Figure 12 shows the turbulent scalar flux $-uc$ and $-vc$ for dense (Φ=0.061) and sparse (Φ=0.015) canopies. The RMS values of the streamwise velocity, u', and the concentration, c', are used to normalize the flux quantities. The turbulent flux $-uc$ has the positive values and $-vc$ has the negative values above the vegetation edge (y/h>1.0). The large peak values of $-uc$ and $-vc$ are located in the over-canopy region. This indicates that the high distribution of concentration (c>0) is transported upward by the ejection motion (u<0, v>0). In contrast, $-uc$ have the negative values within the canopy layer, which implies that the sweep motion (u>0, v<0) transports the dye concentration into the canopy layer (c>0).

It should be noticed that the values of the turbulent scalar flux $-uc$ and $-vc$ are greater for dense canopy than for sparse canopy, which is

consistent with Figure 5. These results reveal that the strong shear layer near the vegetation edge generates the large-scale coherent vortices for dense canopy and larger distributions of the dye concentration are transported toward the over- and within-canopies more significantly.

Figure 13 shows the vertical distribution of turbulent scalar flux $-uc$ at x/L_v=2.0 for dense canopy (Φ=0.061) by using conditional sampling of the Ejections and Sweeps. The bulk mean velocity U_m and the time-averaged concentration C are used to normalize the flux quantities. The turbulent scalar flux $-uc_{Sweep}$ has the larger positive values within the canopy layer than the $-uc_{Non-conditional}$, whereas the values of $-uc_{Ejection}$ become larger above the vegetation edge (y/h=1.2-2.0).

Vertical penetration of turbulent scalar flux into the canopy is a measure of a region within the canopy, which actively exchanges mass. The extent of this region may be defined as the point within the canopy at which the turbulent scalar flux $-uc$ becomes negligibly small. In Figure 13, δ_c is the penetration thickness of turbulent scalar flux. δ_c (Sweep) is significantly larger than δ_c (Non-conditional). This implies that the Sweep motions dominate the vertical penetration of scalar flux into the canopy. This conclusion is supported by the conditional sampling concentration (Figure 11).

4 CONCLUSIONS

This study conducted PIV & LIF measurements to reveal the effects of the submerged vegetation on scalar flux in open-channel flows with rigid vegetations. The nozzle tip position was changed to examine the turbulent diffusion properties in all three sub-zones of the vegetated open-channel flow.

The significant results obtained in this study are as follows:

1. The half-value-width becomes larger in the mixing-layer zone and the vertical diffusion is smaller in the wake zone and in the log-law zone. This implies that a large-scale coherent vortex is generated near the vegetation edge and the vertical turbulent exchange contributes largely to the scalar transport in the mixing-layer zone.
2. On the basis of LIF&PIV data, the effect of the coherent motion on mass transport was examined quantitatively. The conditional analysis reveals that the large distributions of dye concentration are transported toward the above-canopy and the within-canopy regions by ejection and sweep motions, respectively.
3. The PIV-LIF measurements afford us to calculate the local covariance between concentration and velocity fluctuations. The values of the turbulent scalar flux are greater for dense canopy than those for sparse canopy. These results reveal that the strong shear layer near the vegetation edge generates the large-scale coherent vortices for dense canopy and larger distributions of the dye concentration are transported toward the over- and within- canopies more significantly.

REFERENCES

Chen, D., and Jirka, G.H. 1999. LIF study of plane jet bounded in shallow water layer. J. Hydraul. Eng., 125, 817-826.

Crimaldi, J. P. and Koseff, J. R. 2001. High-resolution measurements of the spatial and temporal scalar structure of a turbulent plume, Experiments in Fluids, 31, 90-102.

Gao, W., Shaw, R.H. and Paw, K.T. 1988. Observation of organized structure in turbulent flow within and above a forest canopy. Boundary-Layer Meteorology, 47, 349-377.

Ghisalberti, M. and Nepf, H. 2005. Mass transfer in the vegetated shear flows. Environ. Fluid Mech., 5(6), 527-551.

Jamali, M., Zhang, H. and Nepf, H. 2008. Exchange flow between canopy and open water, J. Fluid Mech., 611, 237-254.

Nepf, H., and Vivoni, E. R. 2000. Flow structure in depth-limited vegetated flow, J. of Geophys. Res.105, 28547-28557.

Nezu, I., and Sanjou. M. 2008. Turbulence structure and coherent motion in vegetated canopy open-channel flows. J. of Hydro-environment Res.. 2, 62-90.

Poggi, D., Porpotato, A. and Ridolfi, L. 2004. The effect of vegetation density on canopy sub-layer turbulence, Boundary-Layer Meteorology, 111, 565-587.

Raupach, M.R., Finnigan, J.J., Brunet, J.J, 1996. Coherent eddies and turbulence in vegetation canopies: the mixing layer analogy, Boundary Layer Meteor., 78, 351-382.

Rahman, S., and Webster, D.R. 2005. The effect of bed roughness on scalar fluctuations in turbulent boundary layers, Experiments in Fluids, 38, 372-384.

Reidenbach, M.A., Koseff, J.R, and Monismith, S.G. 2007: Laboratory experiments of fine-scale mixing and mass transport within a coral canopy, Physics of Fluids, 19, 075107.

Webster, D.R., Rahman, S., and Dasi, L.P. 2003. Laser-induced fluorescene measurements of a turbulent plume, J. Eng. Mech., 129,1130-1137.